Chalcogenide Letters Vol. 8, No. 9, September 2011, p. 561-569

REFLECTIVE CHARACTERISTICS OF Ni DOPED ZnS NANOPARTICLE-PIGMENT AND THEIR COATINGS

SANJEEV KUMAR[a*], N.K. VERMA[a], M.L. SINGLA[b]
[a]*Nano Research Lab, School of Physics and Materials Science, Thapar University, Patiala 147 004, India.*
[b]*Central Scientific Instruments Organisation, Chandigarh 160 030, India.*

The influence of Ni concentration (0 – 0.100%) on the reflective properties of ZnS nanoparticle-pigment as well as on their reflective coatings has been investigated. ZnS nanoparticles synthesized via chemical precipitation method were characterized by using X-ray diffraction (XRD), energy dispersive X-ray spectroscope (EDS), scanning electron microscope (SEM), transmission electron microscope (TEM), UV-Vis absorption, fluorospectrophotometer, and UV-Vis diffuse reflectance spectroscopy (UV-Vis DRS). It has been found that with the increase in the dopant concentration form 0 – 0.100%, the crystallite of ZnS particles changes from 10.00 to 3.01 nm and photocatalytic activity decreases. The structure and morphology remains virtually unchanged as well as no absorption edge in absorption spectra and luminescent peak in the luminescent spectra was observed due to doping. On comparing the diffuse reflectance, ZnS nanoparticles with 0.005% Ni, found to possess maximum diffuse reflectance, 92.51 - 97.77%. Employing these nanoparticles as reflective pigment, coating material was prepared and applied on aluminium substrate with different coating thicknesses to develop reflectors. These reflectors show maximum diffuse reflectance, 98.72 - 99.43%, for the 0.2 mm thick coating.

(Received August 17, 2011; accepted September 20, 2011)

Keywords: ZnS nanoparticles; Doping; Coatings; Reflectors, UV-visible diffuse reflectance spectroscopy

1. Introduction

II-VI semiconductors such as ZnS, CdS, ZnO, CdTe are the foremost promising materials and much in demand for optical and optoelectronic applications [1-3]. Among these semiconductors ZnS has wide band-gap energy of 3.68 eV for bulk cubic phase and 3.80 eV for bulk hexagonal phase [4]. Due to large band gap, ZnS is an essential phosphor host lattice material for electroluminescent devices. It is one of the most important materials in photonics owing to its high transmittance in visible region and high index of refraction (about 2.2) [5]. It has been used as a reference material to test several theoretical models in condensed matter physics [6].

ZnS nanoparticles capped with cetyltrimethylammonium bromide, thioglycerol, ethylene glycol, methacrylic acid, polyvinyl pyrrolidone have been prepared, respectively, using microemulsion, hydrothermal, solvolthermal/hydrothermal, sol-gel, chemical vapor deposition [7-11]. These nanoparticles are much sought-after for applications in CRT screens, catalysts, optical waveguides, reflectors, anti-reflecting films, etc. [12-15]. Different types of dopants with different concentrations have been used to enhance the optical properties of ZnS nanoparticles. These nanoparticles doped with optically active centers have been found useful in fluorescent bio-labeling [16] whereas, those doped with transition metal ions or rare earth ions used as phosphors [17] [10]. Investigations have also been made on the photophysical and photochemical properties of ZnS nanomaterials doped with Cu, Co, Eu, Ce, Mn, Ag and Er [18-20]. Keeping the above points in view, considerable experimental work has been performed in the past in order to

*Corresponding author: kumarsanju25@gmail.com

synthesize and understand the properties of ZnS nanoparticles with/without capping agent and dopant, for various applications.

One of the applications of ZnS is in reflective coatings. A reflective coating is an engineered formulation of pigment, binder, solvent and additives that mix to create a specific product with its own reflective characteristics [21]. Reflective pigment: a particulate solid that is dispersed in coating material to provide certain characteristics to it, including colour, opacity, durability, mechanical strength and corrosion protection for metallic substrates. ZnS is used as reflective pigment in the coating industry due its high index of refraction and large band gap. In industry, ZnS is prepared by reacting its respective mineral ores; after crushing, aggregated crystals are shattered into small granules. This results in individual particles of irregular shape and size. Not only do the particles vary in shape and size, but also in their composition [22]. ZnS particles so obtained are unstable to visible light and get decolourized. To avoid the decolourization, doping of ZnS with cobalt is done [12]. But due to this doping a large absorption edge in the range 650 to 700 nm is developed in ZnS, so it cannot be used as white reflective pigment in the industry. But the above mentioned problems can be solved by (a) creating a novel ZnS pigment with unique crystal structure, morphology and surface chemistry (b) preventing the decolourization of ZnS by doping it with dopant which does not produce absorption edge in the visible region and can also control the morphology (c) functionalizing ZnS surface with surfactant such that it can control the morphology of particles as well as avoid its decolourization.

In this paper, we are going to present the research work in the area, in which, to the best of our knowledge, no one has reported earlier. The research work includes synthesis of thioglycerol capped Ni-doped ZnS nanoparticle-pigment; effect of Ni concentration on their photo-catalytic and reflective properties; and study on the diffuse reflectance of ZnS nanoparticle-based reflectors.

2. Experimental

Analytical grade reagents of sodium sulphide (Na_2S), zinc acetate ($Zn(O_2CCH_3)_2$), nickel acetate ($(CH_3CO_2)_2Ni{\cdot}4H_2O$) and thioglycerol ($C_3H_8O_2S$) were procured from SIGMA-Aldrich, whereas acrylic binder (VISYCRYL-8350) from N. R. Chemicals.

Synthesis of undoped/doped ZnS nanoparticles: Undoped and doped ZnS nanoparticles were synthesised by chemical precipitation technique [9, 16], by mixing nickel acetate of different concentrations, 0 to 0.100%, with zinc acetate aqueous solution. To this solution, sodium sulphide aqueous solution was also added drop-wise, followed by thioglycerol, to prevent agglomeration of the particles. The precipitates were washed and dried. The undoped and Ni-doped ZnS nanoparticles, so obtained, were finally crushed to the powder form.

Preparation of coating material and reflectors: Coating material was prepared by dispersing ZnS: Ni nanoparticles (also called pigment) and acrylic binder in distilled water, using planetary ball running at 1000 rpm for five minutes. pH of the coating was adjusted to 7. The adjustment of the pH in coating material is important in order to maintain stable pigment dispersion, to reduce biological growth and in general, to optimize the performance of coating material during storage and application. The aluminium sheets, used as substrates, were cleaned mechanically and ultrasonically for making reflectors. The cleaning of the sheets is very important to ensure that the coating material meets the required quality standards for appearance, adhesion and corrosion resistance. Before applying the coating material, a thin layer of binder was applied to the substrate for better resistance to corrosion and adhesion. The reflectors were then made by applying two layers of coating, one over the other; care was taken to apply the second layer only after the glossy appearance of the first layer disappeared.

PANanalyticals X'Perto Pro X-ray diffractometer was employed to determine phase purity and crystal structure of the synthesised nanoparticles. Doping of Ni in ZnS was confirmed by energy dispersive x-ray (EDX) spectroscopy using NORAN System Six. Size and morphology of the nanoparticles were studied through Hitachi (H-7500) transmission electron microscope (TEM) and JEOL (JXA-8200) scanning electron microscope (SEM). Perkin Elmer (350) UV-Visible spectrophotometer was used to record optical absorption spectra and, Cary Varian fluorospectrophotometer, to measure PL.

Measurement of diffuse reflectance: UV-Visible spectrophotometer, attached with integrating sphere to spatially integrate the radiant flux, was used to measure diffuse reflectance of the nanoparticles. For this measurement, the nanoparticles were pressed into thick pellets, and placed at the entrance port of the integrating sphere. The same set up was used to measure diffuse reflectance of the developed reflectors. Calibration of the reflectance scale was done by standard reference material (WS-1-SL, Spectralon).

Photocatalytic degradation: A 500 ml reagent beaker was used as a batch reactor for the study. The illumination was provided by Philips 15 W compact fluorescent lamp (CFL). To study photocatalytic activity, a known concentration of the catalyst (ZnS:Ni) was dispersed in methyl orange dye. This solution was first placed in dark for one hour to reach a state of adsorption equilibrium, and, then, illuminated with a visible-light source of 10,000 lux. Just after illumination, samples (5 ml each) were taken out after every hour, and these were used for recording UV-visible spectra of the dye. The spectra absorption peak from 450 to 500 nm was monitored to carry out degradation analysis of ZnS:Ni.

3. Results and discussion

Many synthetic methods are available for the synthesize ZnS nanoparticles with various shapes and sizes [7-11]. To fully utilize the functional properties of the nanoparticles, well dispersed systems are desirable. Recently, chemical precipitation has been widely used for the synthesis of semiconductor nanomaterials because of their easy control over reaction parameter. By changing the reaction conditions, for example the concentration of precursors, the nature of solvent, pH of the reaction mixture, reaction temperature, suitable capping agent and dopant, it is possible to synthesis a variety of nanoparticles with different morphology keeping intact the monodispersity.

Fig. 1 shows the X-ray diffraction pattern of undoped and doped ZnS nanoparticles. The XRD peaks have been found to correspond to (111), (220), and (311) planes of the pure ZnS cubic phase (JCPDS 05-0566). The characteristic peaks of the incorporated Ni were not present, which indicate the good dispersity of the incorporated dopant. The structure of ZnS remains virtually unchanged by the incorporation of the dopant but the peaks got broadened. Broadening of undoped and doped samples indicates the formation of ZnS nanocrystals. The nanocrystals have lesser lattice planes compared to bulk, which contributes to the broadening of peaks in the diffraction pattern.

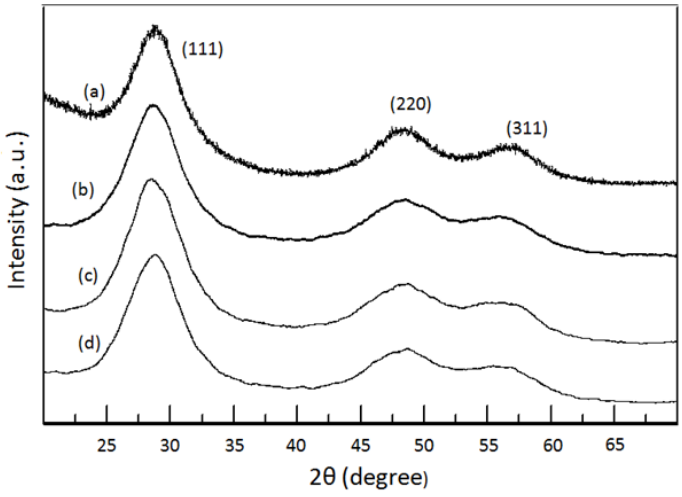

Fig. 1 X-ray diffraction patterns of (a) 0% (b) 0.003% (c) 0.005% (d) 0.100% Ni doped ZnS nanoparticles.

The crystallite sizes of the undoped and doped ZnS are determined from the broadening of the main (111) peak by Debey-Scherrer equation (1) [23],

$$d = \frac{0.91\lambda}{\beta \cos\theta} \tag{1}$$

where d is the crystallite size; λ, the wavelength of X-rays; , the full width at half maximum (FWHM) of the diffraction peak and θ, the Bragg's angle. The full width at half maximum (FWHM) has been calculated from the most intense peak (Fig. 1), using Lorentz best fit curve (R^2 > 0.98). Table 1 shows the crystallite sizes of the samples, calculated using Debye Scherrer's equation. It is clear from Table 1 that with increase in Ni concentration, the crystallite size decreases.

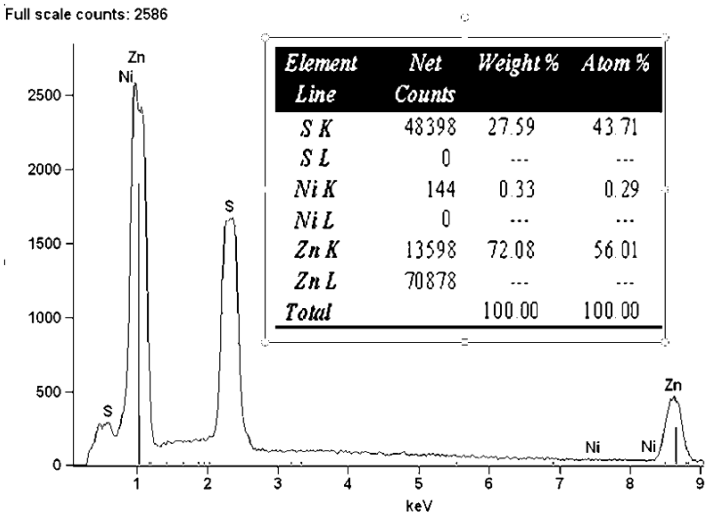

Element Line	Net Counts	Weight %	Atom %
S K	48398	27.59	43.71
S L	0	---	---
Ni K	144	0.33	0.29
Ni L	0	---	---
Zn K	13598	72.08	56.01
Zn L	70878	---	---
Total		100.00	100.00

Fig. 2 EDX spectra of ZnS doped with 0.100% of Ni.

The composition analysis of the ZnS: Ni nanoparticles, was carried out by EDX spectroscopy. Fig. 2 shows the EDX spectrum of 0.100% Ni-doped ZnS nanoparticles. Ni-doped ZnS nanoparticles were found to have atomic percentage 56.0 of Zn, 43.71 of S and 0.29 of Ni, which confirms doping of Ni in the host ZnS. The EDX spectra for other Ni-doping concentrations, 0.003% and 0.005%, also corroborate the presence of Ni in ZnS.

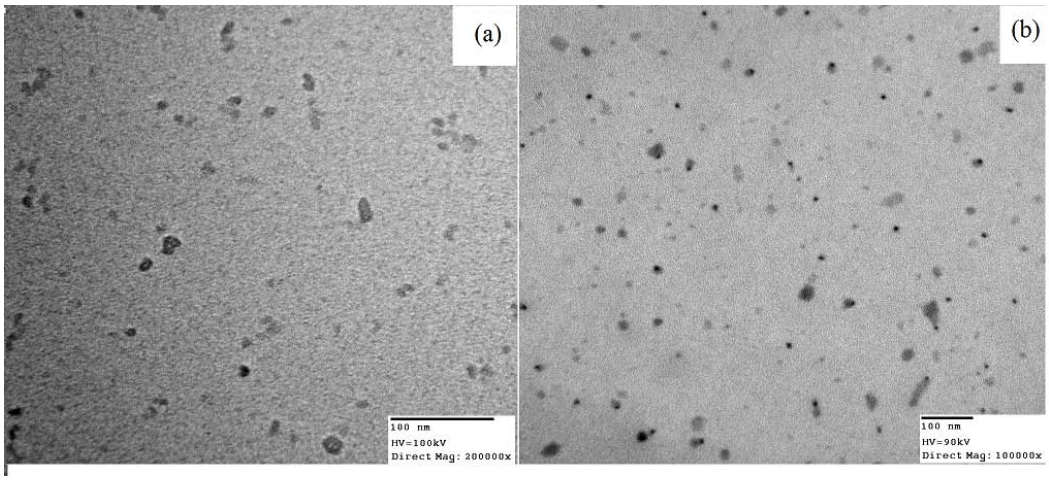

Fig. 3 TEM micrographs of undoped ZnS nanoparticles (a) undoped (b) 0.100% of Ni.

The TEM micrographs of undoped (Fig. 3(a)) and doped (Fig. 3(b)) ZnS nanoparticles show that the nanoparticles are evenly dispersed and nearly spherical with size in the range,

respectively, 25 to 30 nm and 15 to 20 nm, which shows no effect of Ni doping on the morphology of the nanoparticles. The SEM analysis, Fig. 4(a, b) also show spherical symmetry and uniformity of the undoped and doped ZnS nanoparticles.

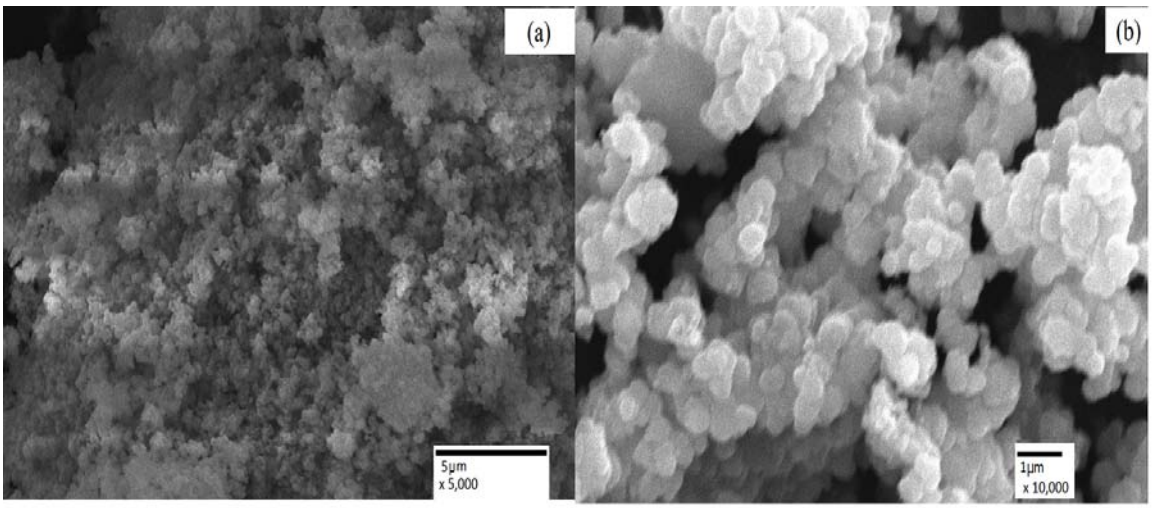

Fig. 4 SEM micrographs of ZnS nanoparticles (a) undoped (b) 0.100% of Ni

Study of materials by means of optical absorption provides a simple method for explaining some features concerning the band structure of materials. The UV-Vis absorption spectra (Fig. 5(a)) of the synthesised ZnS nanoparticles have been recorded, to measure their band-gap.

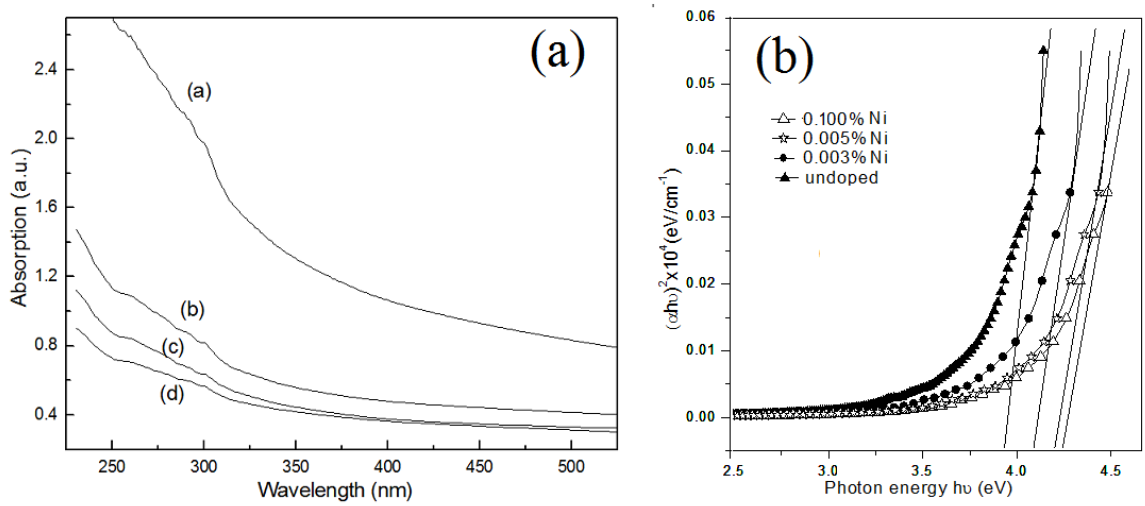

Fig. 5 ***(a)*** *Absorption spectra of (a) 0% (b) 0.003% (c) 0.005% (d) 0.100% Ni doped ZnS nanoparticles* ***(b)*** *Plots of $(\alpha h\nu)^2$ versus hν obtained from the absorption spectra.*

The spectra show absorption edge of the nanoparticles in the range - 300 to 320 nm, showing these nanoparticles being blue-shifted as compared to bulk ZnS for which the peak is at 336 nm [24]. The blue shift in the absorption edge is due to the quantum confinement of the excitons present in the sample, resulting in a more discrete energy spectrum of the individual nanoparticles. The effect of the quantum confinement on impurity depends upon the size of the host crystal. As the size of the host crystal decreases, the degree of confinement and its effect increases [5]. On doping Ni in the ZnS nanoparticles, the blue shift further increases, which might

be due to the fact Ni forming new energy levels in the ZnS energy band. Using Tauc's relation [25], the band-gap of ZnS nanoparticles has been calculated and found to be, 3.90 - 4.20 eV (Fig. 5(b)), Table 1.

Table 1. Crystallite size and band-gap variation with dopant concentration

Sr. No.	Sample	Crystallite size (nm)	Band Gap energy (E_g)
(a)	Undoped ZnS	10.00	3.90eV
(b)	ZnS doped with 0.003% of Ni	8.60	4.00eV
(c)	ZnS doped with 0.005% of Ni	7.23	4.10eV
(d)	ZnS doped with 0.100% of Ni	3.01	4.20eV

Fig. 6 shows the PL spectra of ZnS nanoparticles at an excitation wavelength of 370 nm. A broad luminescence peak at 430 nm is observed for all the samples in the spectra, irrespective of the doping. This peak is attributed to S^{2-} ion vacancies [26]. With increase in the doping concentration, the peak gets broadened and its intensity decreases; this might be due to the interaction between Ni ion and ZnS. Ni provides an effective non-radiative recombination path for the exciton resulting in decreasing its luminescent intensity [27]. The incorporation of Ni in ZnS leads to localized electronic states in the band-gap, which arise from the 3d-shell of Ni ion under the action of surrounding ZnS crystal field [28]. The particles become smaller with increase in doping concentration (as observed in the XRD study) leading to increases in the surface/volume ratio. Due to this surface states corresponding to Ni in ZnS increase which reduces the excitonic emission via nonradiative surface recombination. This indicates that surface states are very important to the optical properties of nanoparticles. The peaks at 486 and 520 nm may be due to the zinc vacancy related defects [25].

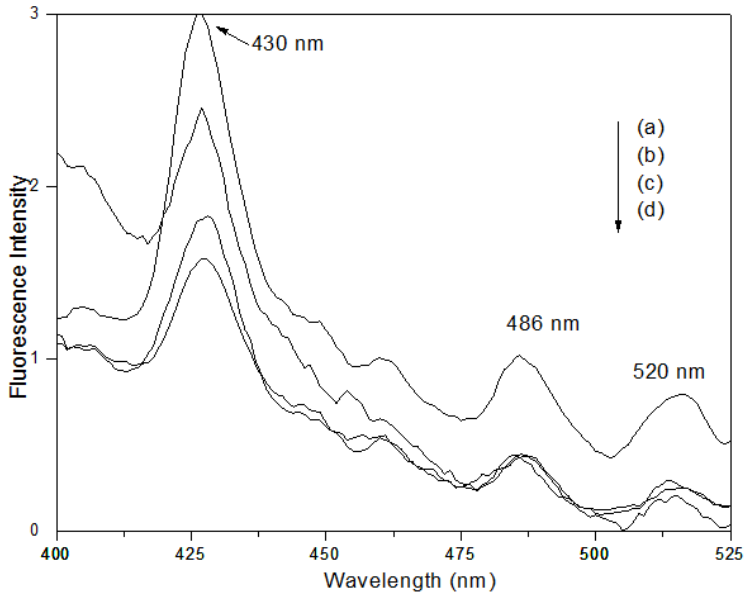

Fig. 6 Photoluminescence emission spectra of (a) 0% (b) 0.003% (c) 0.005% (d) 0.100% Ni doped Zn nanoparticles.

Photodegradation of methyl orange dye was performed to check the photocatalytic activity of ZnS nanoparticles. Influence of various reaction parameters like reaction time, amount of the

catalyst and concentration of the dye is investigated to select an appropriate condition for comparison of photocatalytic activity. The intensity corresponding to the absorption characteristic peak of methyl orange dye at 468 nm is used to analyze the photocatalytic degradation. Fig. 7(a) shows the absorption spectra of a methyl orange aqueous solution exposed to visible light for various times in the presence of ZnS doped with 0.100% of nickel. Absorption spectra reveals that there is little drop in the intensity of peak (at 468 nm) of dye with increasing visible-light exposure time and the intensity of the peak remains almost same after 6 hour. Fig. 7(b) shows the comparison of photocatalytic activities of undoped and doped ZnS samples. It shows a small degradation of the dye for different Ni concentrations. The effective surface area and dispersion stability of ZnS are the two competing effects that determine the photocatalytic activity of Ni doped ZnS in methyl orange dye.

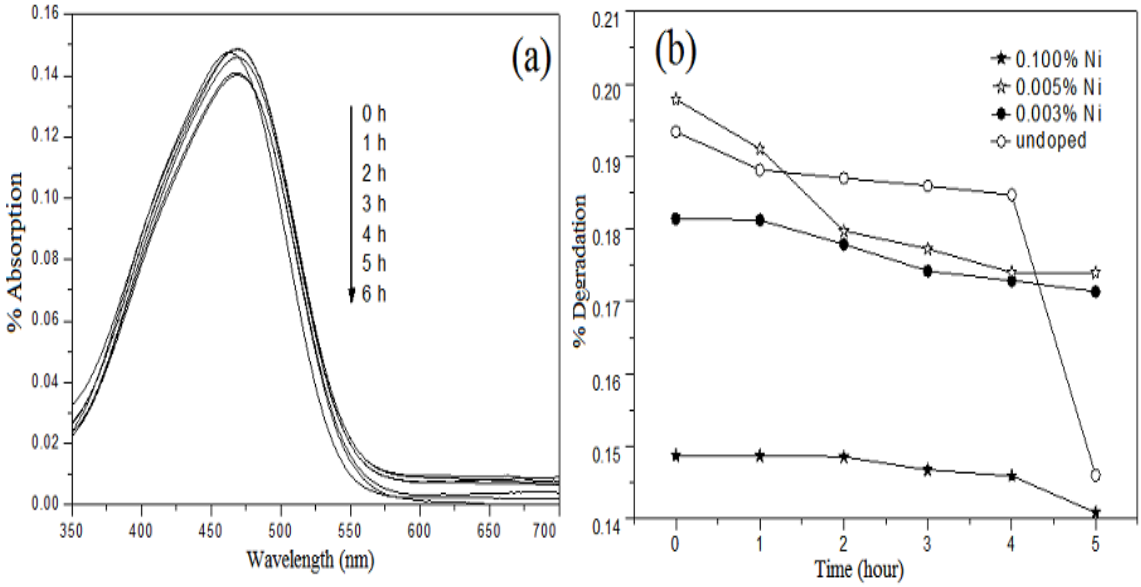

Fig. 7 ***(a)*** *Absorption changes of methyl orange aqueous solution in the presence of ZnS with 0.100% Ni as a function of irradiation time* ***(b)*** *Comparison of photocatalytic activities of (a) 0% (b) 0.003% (c) 0.005% (d) 0.100% Ni doped ZnS nanoparticles for the photocatalytic decolourization of methyl orange dye*

Effective ZnS surface area available for methyl orange would decrease due to incorporation of Ni, which induces decreased photocatalytic activity. That is why the ZnS doped with 0.100% of nickel (curve (d)) shows the lowest adsorption of dye and its initial value of saturation is very low as compared to other samples. Secondly, on the other hand, dispersion stability (Fig. 4(b)), decreased by incorporation of nickel, would also expose the less ZnS surface to methyl orange, may be the reason for low dye degradation. So higher the dopant concentration, less the effective surface of ZnS available for reaction and lower is the degradation of dye. ZnS doped with 0.003% of Ni shows the higher initial saturation value due to lower content of dopant as compared to sample doped with 0.100% of Ni. The samples doped with 0.003% and 0.100% of Ni show similar photocatalytic activity. The sample doped with 0.005% of Ni shows higher initial saturation value; this might be due to the improved dispersion stability by Ni and hence larger available effective surface of ZnS nanoparticles. Thus, the present results offer nickel as the effective dopant for the decreased photocatalytic activity of ZnS.

Fig. 8(a) shows the diffuse reflectance spectra of ZnS nanoparticles. It is clear from the Fig. 8(a) that with the increase in the Ni concentration from 0 to 0.005%, the diffuse reflectance increases from 89.23 - 95.21% to 92.51 - 97.77% which might be due to increase in surface states of Ni ions and decrease in surface defects in ZnS (confirmed by PL study). The diffuse reflectance of 0.005% Ni-doped ZnS nanoparticles has been found to be maximum (92.51 to 97.77%).

Interestingly, the diffuse reflectance decreases, on further increasing the Ni concentration from 0.005 to 0.100%; agglomeration of the ZnS nanoparticles may be responsible for it (Fig. 4(b)). A broad reflectance peak, in the wavelength region, 530 to 600 nm, for 0.100% Ni-doping, corresponds to the dark green to the yellowish portion of the visible region; similar colour change has been noticed even during the synthesis process.

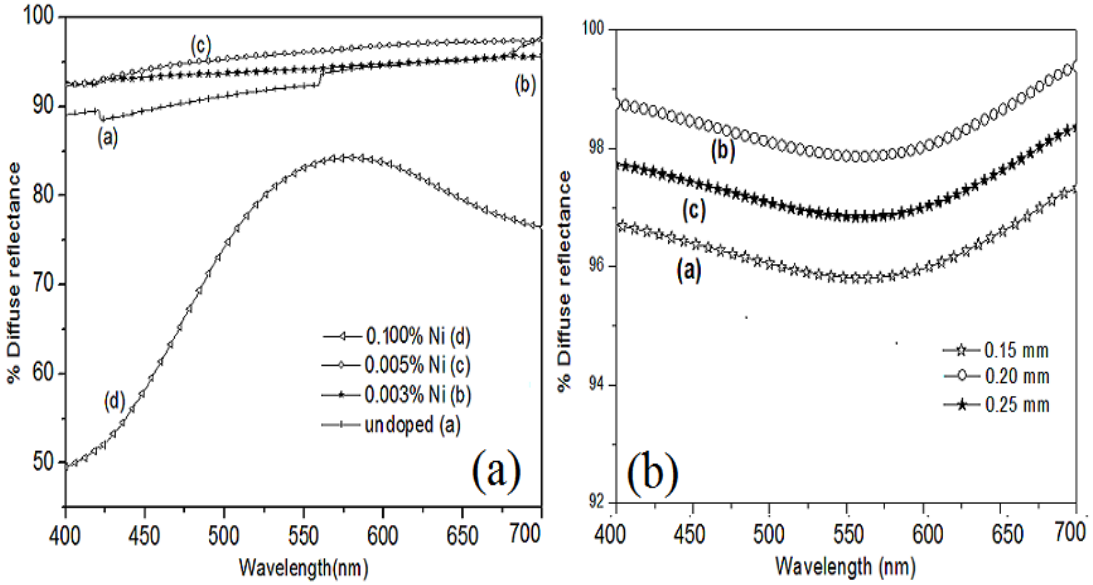

Fig. 8 ***(a)*** *Diffuse reflectance spectra of (a) 0% (b) 0.003% (c) 0.005% (d) 0.100% Ni doped ZnS nanoparticles* ***(b)*** *Diffuse reflectance spectra of the developed reflectors having different coating thicknesses.*

The doping of 0.005% Ni in ZnS nanoparticles shows maximum diffuse reflectance (Fig. 8(a)). Therefore these particles have been employed for the preparation of reflective coatings. Different-thickness coating panels were prepared, and their diffuse reflectance measured. Fig. 8(b) shows diffuse reflectance spectra of reflectors having different coating-thickness. With increase in the coating thickness, i.e., from 0.15 mm to 0.20 mm, there is an increase in the reflectance from 96.70 - 97.34% to 98.72 - 99.43% for the visible region. This is due to the fact that greater the film thickness, greater the number of particles on the substrate, which contribute to the higher reflectance. On further increasing the coating thickness from 0.20 to 0.25 mm, the diffuse reflectance decreases 98.72 - 99.43% to 97.73 - 98.35%. This is because of over pigment coating condition [29]. There is an optimum coating thickness (0.20 m in present case), above and below which the reflectance decreases. At the optimum coating thickness, the critical volume pigment concentration, that's the volume, above or below which a substantial difference in the behaviour and appearance of the coating is observed, plays an important role in determining reflectance. Thus, the coating thickness plays an important role in controlling the diffuse reflectance.

4. Conclusions

ZnS undoped and doped nanoparticles were successfully synthesized and characterized with different characterization techniques. The doped ZnS nanoparticles show little decrease in the photodegradation of the dye; this is, because the dopant reduces the overall ZnS surface area thereby slowing the rate of reaction. The ZnS nanoparticles with 0.005% Ni-doping registered maximum diffuse reflectance - 92.51 to 97.77%, which might be due to increase in Ni surface states in ZnS. Further, the reflectors developed using 0.005% Ni-doped ZnS nanoparticles based coatings materials, also, showed maximum diffuse reflectance, 98.72 to 99.43%, for 0.20 mm thick coating. The developed reflectors find use in almost every situation and area wherever illumination is required.

Acknowledgement

Sanjeev Kumar is grateful to the Department of Science and Technology, Government of India, for awarding him INSPIRE fellowship to carry out the current research work.

Referencess

[1] A. Tiwari, S. A. Khan, R. S. Kher, Adv. Appl. Sci. Res. **2,** 105 (2011).
[2] M. Godlewski, E. Guziewicz, K. Kopalko, G. Luka, M. I. Lukasiewicz, T. Krajewski, B. S. Witkowski, S. Gieraltowska, Low Temp. Phys. **37,** 235 (2011).
[3] R. E. Pimpinella, A. M. Mintairov, X. Liu, T. H. Kosel, J. L. Merz, J. K. Furdyna, M. Dobrowolska, J. Vac. Sci. Technol. B **29**, 1 (2011).
[4] N. Saravanan, G. B. Tec, S. Y. P Yap, K. M. Cheong, J. Mater. Sci. Mater. Electron. **19,** 1206 (2008).
[5] M. J. Pawar, S. D. Nimkar, P. P. Nannukar, A. S. Tale, S. B. Deshmukh, S. S. Chaure, Chalcogenide Letters **7,** 139 (2010).
[6] W. Q. Peng, S. C. Qu, G. W. Cong, Z. G.Wang, Cryst. Growth Des. **6,** 1518 (2006).
[7] S. K. Mehta, S. Kumar, S. Chaudhary, K. K. Bhasin, M. Gradzielski, Nanoscale Res. Lett. **4**, 17 (2009).
[8] M. S. Niasari, F. Davar, M. Mazaheri, J. Alloys Compd. **470,** 502 (2009).
[9] M. P. Anil, S. G. Shivram, J. Crystal Growth, doi:10.1016/j.jcrysgro.2011.01.087 (2011).
[10] L. Q. Yue, F. J. Zhang, J. Z. Huang, L. W. Wang, J. Nanosci. Nanotechnol. **8**, 1199 (2008).
[11] R. Maitya, U.N. Maitia, M.K. Mitrab, K.K. Chattopadhyaya, Physica E **33**, 104 (2006).
[12] G. Buxbaum, G. Pfaff, Industrial Inorganic Pigment, 3rd edn. WILEY-VCH, Weinheim (2005).
[13] H. Zhang, X. Chen, Z. Li, J. Kou, T. Yu, Z. Zou J Phys D: Appl Phys **40**, 6846 (2007).
[14] Z. Feng, H. Hu, S. C. Cent, Eur J. Phys. **7**, 340 (2009).
[15] Y. Wang, N. Herron, N. Mahler, J. Opt. Soc. Am. B **6**, 808 (1989).
[16] E. E. Lees, M. J. Gunzburg, T. L. Nguyen, G. J. Howlett, J. Rothacker, E. C. Nice, H. A. Ckayton, P. Mulvaney, Nano Lett. **8**, 2883 (2008).
[17] A. C. Wright, I. V. F. Viney, Philosophical Magazine B, **81**, 279 (2001).
[18] P. Yang, M. Lu, D. Xu, D. Yuan, C. Song, S. Liu, X. Cheng, Opt. Mater. **24**, 497 (2003).
[19] Y. Zhang, Y. Li, J. Phys. Chem. **108**, 17805 (2004).
[20] K. Singh, S. Kumar, N. K.Verma, H. S. Bhatti, J. Nanopart. Res. **11**, 1017 (2009).
[21] R. Talbert, Paint Technology Handbook, Taylor & Francis Group, London (2008).
[22] G. O'Hanlon, Why some paints are transparent and others opaque, (2010), Hyperlink: http://naturalpigments.com/education/article.asp?ArticleID=8
[23] G. Cao, Nanostructures and Nanomaterials, Imperial College Press, London (2004).
[24] B. Tripathi, Y. K. Vijay, S. Wate, F. Singh, D. K. Avasthi, Solid-State Electron **51**, 81 (2007).
[25] Z. Jindal, N. K.Verma, J. Mater. Sci. **43,** 6539 (2008).
[26] P. H Borse, N. Deshmukh, R. F. Shinde, S. K. Date, S. K. Kulkarni, J. Mater. Sci. **34,** 6087 (1999).
[27] L. Podlowski, R. Heitz, A. Hoffmann, I. Broser, J. Lumin. **53**, 401 (1992).
[28] T. A. Birman, A. M. Gurvich, M. A. Llina, A. A. Shamanov, J. Appl. Spectrosc. **20**, 44 (1974).
[29] A. A. Tracton, Coating Materials and Surface coatings, Taylor & Francis Group, USA (2007).